OH Radical Yields from the Ozone Reaction with Cycloalkenes

Jill D. Fenske,[†] Keith T. Kuwata,[‡] K. N. Houk,[‡] and Suzanne E. Paulson*[,§]

Department of Chemical Engineering, Department of Chemistry and Biochemistry, and Department of Atmospheric Sciences, University of California at Los Angeles, Los Angeles, California 90095-1565

Received: October 11, 1999; In Final Form: May 22, 2000

OH radical formation yields from the reaction of ozone with several cycloalkenes were measured using small amounts of fast-reacting aromatics and aliphatic ethers to trace OH formation. Measured OH yields are much higher than for acyclic analogues. The yields are 0.62 ± 0.15, 0.54 ± 0.13, 0.36 ± 0.08, and 0.91 ± 0.20 for cyclopentene, cyclohexene, cycloheptene, and 1-methylcyclohexene, respectively. Density functional theory calculations at the B3LYP/6-31G(d,p) level are presented to aid in understanding the trends observed. Theory indicates that the OH production from cycloalkenes is largely controlled by the transition states for the cycloreversion of the primary ozonide.

Introduction

Alkenes make up the majority of nonmethane hydrocarbon emissions globally;[1] sources include automobile exhaust, industrial emissions, and plant life. Ozone−alkene reactions occur during both day and night, and are a source of HO_x (HO_x = OH, HO_2, RO_2) radicals, which are important oxidants in the atmosphere. In urban and rural air where concentrations of unsaturated compounds are sufficiently high, ozone−alkene reactions can be a significant, and in some cases dominant, source of new HO_x.[2] Ozone−alkene reactions have been the focus of much excellent research throughout the past several decades (see Atkinson et al.[3] and Paulson et al.[4] for reviews).

Cycloalkenes are present in ambient air in small quantities; ambient measurements for cyclopentene and cyclohexene fall in the range 0.1−6 ppb.[5−8] Cycloheptene and 1-methylcyclohexene offer potential insight into the mechanistic features of ring-opening ozone−alkene reactions. 1-Methylcyclohexene, in particular, is a simple analogue to α-pinene and Δ^3-carene.

In this study, we have used the small-ratio relative-rate method to measure OH radical yields from the ozone reaction with four cycloalkenes (cyclopentene, cyclohexene, cycloheptene, and 1-methylcyclohexene), with accuracies of ±18−25%. The OH radical yield has been measured previously for cyclopentene (0.61 (+0.30−0.20)[9]), cyclohexene (0.68 (+0.34−0.22)[10]), and 1-methylcyclohexene (0.90 (+0.45−0.30)[9]). No previous measurements have been made for cycloheptene.

To aid in the interpretation of the experimental results, we performed density functional theory (DFT) calculations for each cycloalkene, as well as for *cis*- and *trans*-2-butene. The B3LYP/6-31G(d,p) method has been shown to give results in excellent agreement with high-level CCSD(T)/TZ+2P calculations for ethylene ozonolysis.[11] The only theoretical work to date on the ozonolysis of cycloalkenes has been semiempirical predictions of primary ozonide conformations. Bunnelle and Lee[12] used AM1 to study cyclopentene, and Kawamura et al.[13] used PM3 to study methyl- and acetoxy-substituted cyclopentenes and cyclohexenes. Rathman et al.[14] have recently published MP2/6-31G* calculations on *cis*- and *trans*-2-butene ozonolysis.

Mechanism

The reaction of ozone with cycloalkenes involves the 1,3-dipolar cycloaddition of ozone across the double bond. The resulting primary ozonide decomposes to form a carbonyl moiety and a carbonyl oxide moiety.[15] In the gas phase, the exothermicity of the cleavage will give vibrationally excited products. For cyclohexene:

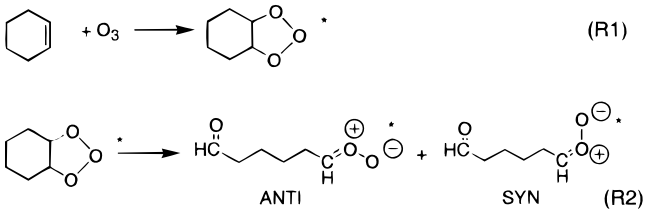

In 1968, Bauld et al.[16] recognized that the decomposition of a primary ozonide produces distinct syn and anti isomers of carbonyl oxide (vide supra). Interconversion between the syn and anti carbonyl oxides is restricted by the partial double-bond character of the C−O bond (see Results). The two isomers have distinct reactivities; syn carbonyl oxides appear to be labile precursors of OH[17−19] (R3−R4), but anti carbonyl oxides will preferentially close to dioxiranes (R5).[17]

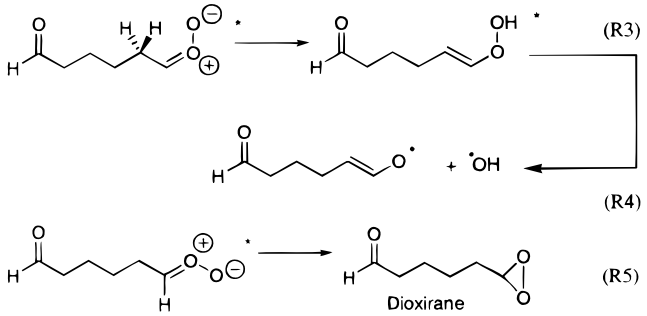

In addition, both isomers may be collisionally thermalized by the surrounding gas. OH radical formation has been measured by several groups, with values ranging from 0.08 to ∼1, depending on the alkene (see Table 1 or Paulson et al.[4]). Donahue et al.[20] observed OH formation directly from ozone−

* To whom correspondence should be addressed.
[†] Department of Chemical Engineering.
[‡] Department of Chemistry and Biochemistry.
[§] Department of Atmospheric Sciences.

10.1021/jp993611q CCC: $19.00
Published on Web 07/15/2000

TABLE 1: Summary of Initial Conditions and Calculated OH Yields

alkene/ tracer	experiment	initial concentration (ppm)	ratio $([Tr]_o/[A]_o)$	Y_{OH} (model)	alkene/ tracer	experiment	initial concentration (ppm)	ratio $([Tr]_o/[A]_o)$	Y_{OH} (model)
cyclopentene	8.11.98	10.0			cycloheptene	6.25.98	9.33		
XYL		1.83	0.183	0.74	TMB		0.833	0.0893	0.32
TMB		0.894	0.0894	0.58	cycloheptene	7.2.98	9.11		
cyclopentene	8.18.98	9.19			TMB		0.805	0.0884	0.34
XYL		1.66	0.181	0.70	cycloheptene	8.12.98	9.24		
TMB		0.834	0.0908	0.58	XYL		1.59	0.172	0.42
cyclopentene	9.4.98	9.01			TMB		0.793	0.0858	0.35
XYL		1.49	0.165	0.62	cycloheptene	8.26.98	9.05		
TMB		0.805	0.0893	—[a]	XYL		1.61	0.178	0.42
cyclopentene	10.28.98	10.9			TMB		0.946	0.104	0.35
XYL		0.361	0.0331	0.62	cycloheptene	8.31.98	9.28		
TMB		0.375	0.0344	0.55	XYL		1.41	0.152	0.42
cyclopentene	11.5.98	9.64			TMB		0.859	0.0926	0.35
XYL		0.410	0.0425	—[a]	cycloheptene	10.26.98	9.98		
TMB		0.244	0.0253	0.56	BUE		0.565	0.0566	0.39
cyclopentene	11.6.98	10.5			TMB		0.420	0.0421	0.32
XYL		0.530	0.050	—[a]	cycloheptene	10.29.98	9.88		
TMB		0.343	0.032	0.57	BUE		0.499	0.0505	0.32
cyclopentene	8.25.98	8.38			TMB		0.342	0.0346	0.30
BUE		1.28	0.153	0.65	***Average***				**0.36 ± 0.03**
TMB		0.810	0.0967	—[a]	MCH[c]	10.22.98	8.55		
cyclopentene	10.27.98	11.2			TMB		0.43	0.050	0.85
BUE		0.566	0.0505	0.69	MCH	8.14.98	12.8		
TMB		0.332	0.0296	—[a]	XYL		1.74	0.136	1.0
Average				**0.62 ± 0.06**[b]	TMB		1.10	0.0863	0.80
cyclohexene	9.17.98	19.7			MCH	10.14.98	13.8		
XYL		0.751	0.0381	—[a]	BUE		0.490	0.0355	1.25
TMB		0.631	0.0320	0.50	TMB		0.271	0.0196	1.0
cyclohexene	9.18.98	18.6			MCH	10.15.98	14.4		
BUE		0.777	0.0419	0.55	BUE		0.623	0.0433	1.25
TMB		0.510	0.0270	0.55	TMB		0.527	0.0366	1.0
cyclohexene	10.6.98	12.8			MCH	10.19.98	13.9		
BUE		0.772	0.0609	0.63	BUE		0.577	0.415	0.92
TMB		0.400	0.0310	0.55	TMB		0.317	0.228	0.80
cyclohexene	10.7.98	9.42			***Average***				**0.91 ± 0.07**
BUE		0.537	0.0573	0.52					
TMB		0.206	0.0220	0.46					
Average				**0.54 ± 0.05**					

[a] Due to co-eluting peaks, the *m*-xylene tracer did not provide reliable data. [b] Reported uncertainties are $2\sigma_m$; σ_m = standard deviation of the mean. [c] MCH = 1-methylcyclohexene.

alkene reactions at low pressure (5 Torr) by laser-induced fluorescence. Olzmann et al.[21] performed master equation analysis to estimate the branching ratios of dioxirane, OH, and thermalized carbonyl oxide formation for ethene and 2,3-dimethyl-2-butene. They predicted branching ratios of ~80%, ~0.2%, and ~20% for dioxirane, OH, and thermalized carbonyl oxide formation, respectively, from ethene ozonolysis at atmospheric pressure; for 2,3-dimethyl-2-butene ozonolysis, they predicted branching ratios of 4%, 70−80%, and 20−30% for dioxirane, OH, and thermalized carbonyl oxide formation, respectively, at atmospheric pressure. These calculations thus predict that more dioxirane is formed from the unsubstituted carbonyl oxide, and more OH is formed from substituted carbonyl oxides.

Hatakeyama et al.[22] have reported yields of thermalized carbonyl oxides, hereinafter referred to as thermalized Criegee intermediates (TCI) due to the uncertainty in the structure of this molecule. They inferred TCI formation from yields of H_2SO_4 in ozone−alkene experiments in the presence of excess SO_2. TCI yields from cyclic compounds with unsubstituted endocyclic double bonds were very low; 0.052, 0.032, and 0.029, from cyclopentene, cyclohexene, and cycloheptene, respectively. Yields for compounds with methyl-substituted endocyclic double bonds are somewhat higher; 1-methylcyclohexene and α-pinene were measured at 0.104 and 0.125, respectively. Exocyclic double bonds give higher yields; methylenecyclohexane and β-pinene yields are 0.216 and 0.249, respectively.[22] Hatakeyama et al. proposed that formation of a cyclic secondary ozonide might explain the low yields of thermalized carbonyl oxide for endocyclic alkenes:

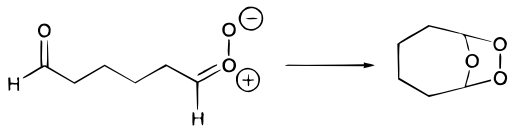

(R6)

Hatakeyama et al.[22] report no direct experimental evidence for the formation of these species, but Bunnelle and Lee[12] observed secondary ozonides from cycloalkene ozonolysis in the liquid phase.

Bunnelle and Lee[12] present experimental evidence that cyclopentene forms a high yield of syn carbonyl oxide, and cyclohexene gives mostly anti carbonyl oxide. Using AM1 calculations, Bunnelle and Lee found that the most stable conformation of the cyclopentene primary ozonide is exo/endo (i.e., the C−C−C flap is exo, and the O−O−O flap is endo), and assert that the structure of the transition state is very similar to the primary ozonide, resulting in cleavage to the syn carbonyl oxide (a "least-motion" transition state). They use similar arguments about the structures of the primary ozonide and transition state to explain the high yields of anti carbonyl oxide from cyclohexene.

Technique to Measure OH Yields

Measuring OH formation is complicated by the high reactivity of alkenes with OH radicals compared with most other compounds. Alkenes react with OH at nearly gas kinetic rates ($6.7-9.4 \times 10^{-11}$ $cm^3molec^{-1}s^{-1}$ for the cycloalkenes studied here[3]). It is possible to scavenge most (i.e., >95%) of the OH with a compound (hereafter referred to as the "tracer") that reacts rapidly with OH but very slowly with O_3. To scavenge the majority of OH, the tracer must be present in large excess (10−1000 times the alkene concentration, depending on the alkene−tracer combination). Under these conditions, deriving the OH yield from the amount of tracer reacted requires measuring small differences between large numbers, which produces large uncertainties in the OH yield.

In this study, we use the small-ratio, relative-rate technique, which has been discussed in detail elsewhere.[23] When the tracer is present in low concentrations (i.e., <10% of the alkene concentration), most of the OH reacts with the alkene rather than the tracer. Under these conditions, up to 30% of the tracer may be consumed, depending on the OH radical rate coefficient of the tracer:

$$O_3 + \text{alkene} \xrightarrow{k_{O_3}} y_{OH}\,OH + y_{OH}\,\text{Dialdehyde}-RO_2 + \text{other products} \quad \text{(R7)}$$

$$OH + \text{alkene} + M \xrightarrow{k_A} RO_2 + M \quad \text{(R8)}$$

$$OH + \text{tracer} + M \xrightarrow{k_{Tr}} R'O_2 + M \quad \text{(R9)}$$

1,3,5-Trimethylbenzene (TMB), *m*-xylene (XYL), and di-*n*-butyl ether (BUE) were chosen as tracers. An OH yield may be derived from an analytical expression obtained from solving R7−R9, but the most accurate way to calculate the OH yield is by solving the ordinary differential equations that describe the chemistry of the complete system, including the reactions of the products, wall losses, and so forth. The analytical and numerical solutions generally fall within 20% of one another.[23] The data in this study were analyzed numerically.

Experimental Description

Experiments were carried out in pillow-shaped 250-L Teflon chambers at 296 ± 2 K. These chambers were equipped with a Teflon tube "injector" (a length of 1/4" Teflon tubing with holes at intervals) to reduce sample mixing time. Chambers were placed in a dark enclosure to eliminate any possible photochemistry. A stream of zero-air (Thermo Environmental Model 111) flushed evaporated liquid hydrocarbons into the chamber as it was filled. Hydrocarbons were used as received from Aldrich, with stated purities as follows: cyclopentene (99.5%), cyclohexene (99+%), cycloheptene (97%), 1-methylcyclohexene (97%), 1,3,5-trimethylbenzene (98%), di-*n*-butyl ether (99.3%), and *m*-xylene (99+%). Ozone was generated in aliquots by flowing pure O_2 through a mercury lamp ozone generator (JeLight PS-3000−30). To ensure that the chamber contents were well mixed, we allowed 30−45 min before determining the initial concentrations. A series of ozone aliquots were added over a period of 6−7 h, each immediately after a gas chromatography (GC) sample injection to allow maximum time before the next sample injection (15−30 min depending on the temperature program used). A gas chromatograph/flame ionization detector (GC/FID; Hewlett-Packard 5890), equipped with either a 30 m × 3 μm × 0.53 mm i.d. DB-624 column or a 30 m × 3 μm × 0.32 mm i.d. DB-1 column (J&W), a 2-mL sample loop, and a computer-controlled injection valve (Valco), monitored the hydrocarbon concentrations throughout the experiments. The GC was calibrated daily with a cyclohexane standard (Scott Specialty Gases). For the other hydrocarbons, the FID response was normalized to the cyclohexane calibration using the number of carbon atoms in the compound of interest. The repeatability of the GC measurements is >0.5% for the same sample. This value overestimates the precision, however, because an FID can drift by 1−2% over several hours. In addition, small product peaks growing near or under the main peaks in a chromatogram as the experiment progresses can significantly reduce the precision of the measurement for points at higher alkene conversion. This problem is particularly acute for cycloalkenes. We attempted to resolve coeluting peaks by changing the column and temperature program, which worked well for cyclohexene, cycloheptene, and 1-methylcyclohexene. For cyclopentene, some peaks were never completely resolved, and the resulting error is reflected in the uncertainty reported for the OH yield. The best results were obtained with the following columns and temperature programs (all temperatures in °C): cyclopentene: DB-1, 0.2 min @ −25, −25−100 @ 30 °C/min, 100−180 @ 15 °C/min, and 2 min @ 180; cyclohexene: DB-624, 0.2 min @ −25, −25−110 @ 20 °C/min, 1 min @ 110, 110−180 @ 30 °C/min, and 1 min @ 180; cycloheptene and 1-methylcyclohexene: DB-624, 0.2 min @ −25, −25−100 @ 30 °C/min, 100−180 @ 15 °C/min, and 2 min @ 180. Initial concentrations are summarized in Table 1.

Theoretical Methods

The geometries and energies of minima and transition structures were determined using density functional theory, employing the Becke3LYP hybrid functional[24] and the 6-31G(d,p) basis set.[25,26] Diradical species were treated with unrestricted Becke3LYP (UB3LYP) theory, using wave functions of broken spin symmetry. We obtained room temperature (298 K) enthalpies and entropies by scaling the (U)B3LYP/6-31G(d,p) harmonic frequencies by a factor of 0.963.[18] The B3LYP/6-31G(d,p) method has been shown to give predictions for ozonolysis reactions in excellent agreement with high-level CCSD(T) calculations.[11,27] In preliminary calculations on ethene ozonolysis, we found that B3LYP/6-31G(d,p) calculations gave activation enthalpies within ±2 kcal/mol of QCISD(T)/6-31G(d,p) predictions. In addition, we examined basis set effects for *cis*-2-butene and *trans*-2-butene with single-point B3LYP/6-311++G(d,p) calculations at the B3LYP/6-31G(d,p) geometries. All results reported here were obtained with the Gaussian 94[28] and Gaussian 98[29] suites of programs.

Results

In most of the experiments described here, we have added pairs of tracers to provide two data sets from which to calculate the OH yield. Because XYL and BUE elute very close to one another, TMB was used together with either XYL or BUE. The tracer pair concentrations may be plotted according to E1:

$$\frac{k_{Tr_1}}{k_{Tr_2}} = \frac{\ln([Tr_1]_o/[Tr_1]_t)}{\ln([Tr_2]_o/[Tr_2]_t)} \quad \text{(E1)}$$

where k_{Tr_i} and $[Tr_i]$ are the OH reaction rate constants and concentrations, respectively, for the i^{th} tracer, provided that the tracers are reacting with OH rather than a different reactive intermediate.[30] For those experiments for which neither tracer was confounded by a coeluting peak (14 experiments), the slopes were 2.3 ± 0.1 and 1.8 ± 0.2 for k_{TMB}/k_{XYL} and k_{TMB}/k_{XYL},

TABLE 2: Rate Coefficients for the OH and O_3 Reactions with Alkenes and Tracers

compound	reaction partner	rate constant ($cm^3 molec^{-1} s^{-1}$)	reference
cyclopentene	OH	6.70×10^{-11}	a
	O_3	5.70×10^{-16}	a
cyclohexene	OH	6.77×10^{-11}	a
	O_3	8.14×10^{-17}	a
cycloheptene	OH	7.40×10^{-11}	a
	O_3	2.45×10^{-17}	a
1-methylcyclohexene	OH	9.40×10^{-11}	a
	O_3	1.65×10^{-16}	a
1,3,5-trimethylbenzene	OH	5.73×10^{-11}	b
m-xylene	OH	2.20×10^{-11}	b
butyl ether	OH	2.88×10^{-11}	b

[a] Recommended value from Atkinson[3]. [b] Kramp and Paulson[31].

respectively. These values are in good agreement with the ratios of the rate coefficients for the tracers reacting with OH ($k_{TMB}/k_{XYL} = 2.4-2.6$ and $k_{TMB}/k_{BUE} = 2.0$[31,3]).

Data analysis was performed by solving the set of ordinary differential equations that describe the chemistry specified in the following way: The cycloalkenes were assumed to react with ozone analogously to other large alkenes (R10−R13), with the recommended rate coefficients from the review by Atkinson.[3] The OH reaction with these cyclic compounds was assumed to be analogous to OH reaction with straight-chain alkenes.[32] The OH formation pathway was assumed to generate dialdehyde−RO_2 radicals (after the alkoxy radical (R4) adds oxygen). These radicals were assumed to react with the same rates as secondary beta-hydroxy alkoxy radicals. The remainder of the carbonyl oxides were assumed to decompose analogously to CH_3CHOO, as recommended by Atkinson,[3] forming such products as HO_2, CO, CO_2, and RO_2 radicals. The RO_2 chemistry is from Jenkin and Hayman[33] and Lightfoot et al.[34] Reactions of common products, RO_2 radicals, and tracers are listed in detail in Paulson et al.[23] Table 2 shows a summary of the rate constants used in this study. The products assumed for the best fit for the O_3 reactions are as follows:

cyclopentene + O_3 →
0.62 $CH(O)(CH_2)_2CH(OO\cdot)CH(O)$ + 0.62 OH +
0.23 $HC(O)(CH_2)_2CH_2OO\cdot$ + 0.10 C_4-aldehyde +
0.32 CO_2 + 0.27 HO_2 + 0.04 CO + 0.04 C_4-dialdehyde (R10)

cyclohexene + O_3 →
0.54 $CH(O)(CH_2)_3CH(OO\cdot)CH(O)$ + 0.54 OH +
0.28 $HC(O)(CH_2)_3CH_2OO\cdot$ + 0.12 C_5-aldehyde +
0.40 CO_2 + 0.34 HO_2 + 0.05 CO + 0.05 C_5-dialdehyde (R11)

cycloheptene + O_3 →
0.36 $CH(O)(CH_2)_4CH(OO\cdot)CH(O)$ + 0.36 OH +
0.40 $HC(O)(CH_2)_4CH_2OO\cdot$ + 0.17 C_6-aldehyde +
0.56 CO_2 + 0.47 HO_2 + 0.08 CO + 0.08 C_6-dialdehyde (R12)

1-methylcyclohexene + O_3 →
0.50 $CH(O)(CH_2)_3CH(OO\cdot)C(O)CH_3$ +
0.41 $CH(O)C(OO\cdot)(CH_2)_3C(O)CH_3$ + 0.91 OH +
0.04 $CH_3C(O)(CH_2)_3CH_2OO\cdot$ +
0.01 $CH_3(CH_2)_3C(O)CH_3$ + 0.03 CO_2 + 0.03 HO_2 (R13)

The calculated OH yields are most sensitive to the OH rate constant of the tracer; any uncertainty in this value is directly translated into the OH yield uncertainty. The uncertainties in the rate coefficients of TMB, XYL, and BUE are not more than ±12%.[31] Paulson et al.[23] showed that for propene, a 10% difference in the OH−alkene reaction rate constant results in a <1% difference in the calculated OH yield.

An additional source of OH radicals is the reaction of HO_2 with O_3. However, calculations indicate that setting all other reactions of HO_2 to zero so that all HO_2 formed reacts only with O_3 has a negligible effect on the calculated OH yield. Thus, HO_2 reaction with O_3 is not a major source of OH in these experiments.

The yields of OH are not particularly sensitive to assumptions made about the product distribution, which affect the analysis to the degree to which the products compete with the alkene and tracer for OH radicals.[23] Although the uncertainties in the products from the ozone−alkene reactions studied here are high, cyclopentene, cyclohexene, cycloheptene, and 1-methylcyclohexene all react rapidly with OH. Because the products do not contain C−C double bonds and thus are not likely to react with OH at rates faster than 2×10^{-11} cm^3 $molec^{-1}s^{-1}$, uncertainties in the OH yield resulting from errors in the product yields will be minimal. Consistent with this idea, for cyclohexene, a 50% decrease in the yield of RO_2 radicals (probably a reasonable estimate of the uncertainty) resulted in an 8% decrease in the OH yield, and a 90% change in the yield of HO_2 radicals resulted in a negligible change in the OH yield. A 2-fold increase in the aldehyde yield resulted in a 3% increase in the calculated OH yield. Thus, for these experiments, we include a ±20% systematic uncertainty in our total reported uncertainty for the OH radical yield to account for uncertainties in rate coefficients and product yields.

Selected data for cyclopentene, cyclohexene, cycloheptene, and 1-methylcyclohexene are shown in Figure 1, panels a−d, and the calculated OH yields for these compounds are shown in Table 1. Calculations were made for each experiment, adjusting only the assumed OH yield to obtain a fit of the data. The best fit OH yields were determined by minimizing the squares of differences between the model-calculated curve and the experimental data. The average calculated OH yield with uncertainties resulting from a combination of observed random error and a ±20% systematic uncertainty are 0.62 ± 0.15, 0.54 ± 0.13, 0.36 ± 0.08, and 0.91 ± 0.20 for cyclopentene, cyclohexene, cycloheptene, and 1-methylcyclohexene, respectively.

Our measurement for cyclopentene (0.62 ± 0.15) is in excellent agreement with the measurement by Atkinson et al. (0.61, +0.30−0.20[9]). Our value for cyclohexene (0.54 ± 0.13) is within the mutual uncertainties of the values measured by Atkinson and Aschmann (0.68, +0.34−0.22[10]), but is significantly lower. The trend of decreasing OH yields shown by our measurements of the cyclopentene−cycloheptene series is the reverse of that suggested by the measurements for cyclopentene and cyclohexene by Atkinson et al.[9,10] For 1-methylcyclohexene, our result (0.91 ± 0.20) is, again, in excellent agreement with that of Atkinson et al. (0.90, +0.45−0.30[9]).

Table 3 lists the activation enthalpies and entropies for the concerted cycloreversion of primary ozonides to produce either anti or syn carbonyl oxides. The transition states we have located (Figures 2−7) are all quite similar. Activation enthalpies range from 14 to 20 kcal/mol, and activation entropies range from −1.3 to +1.8 cal/(mol K). In all of the transition structures,

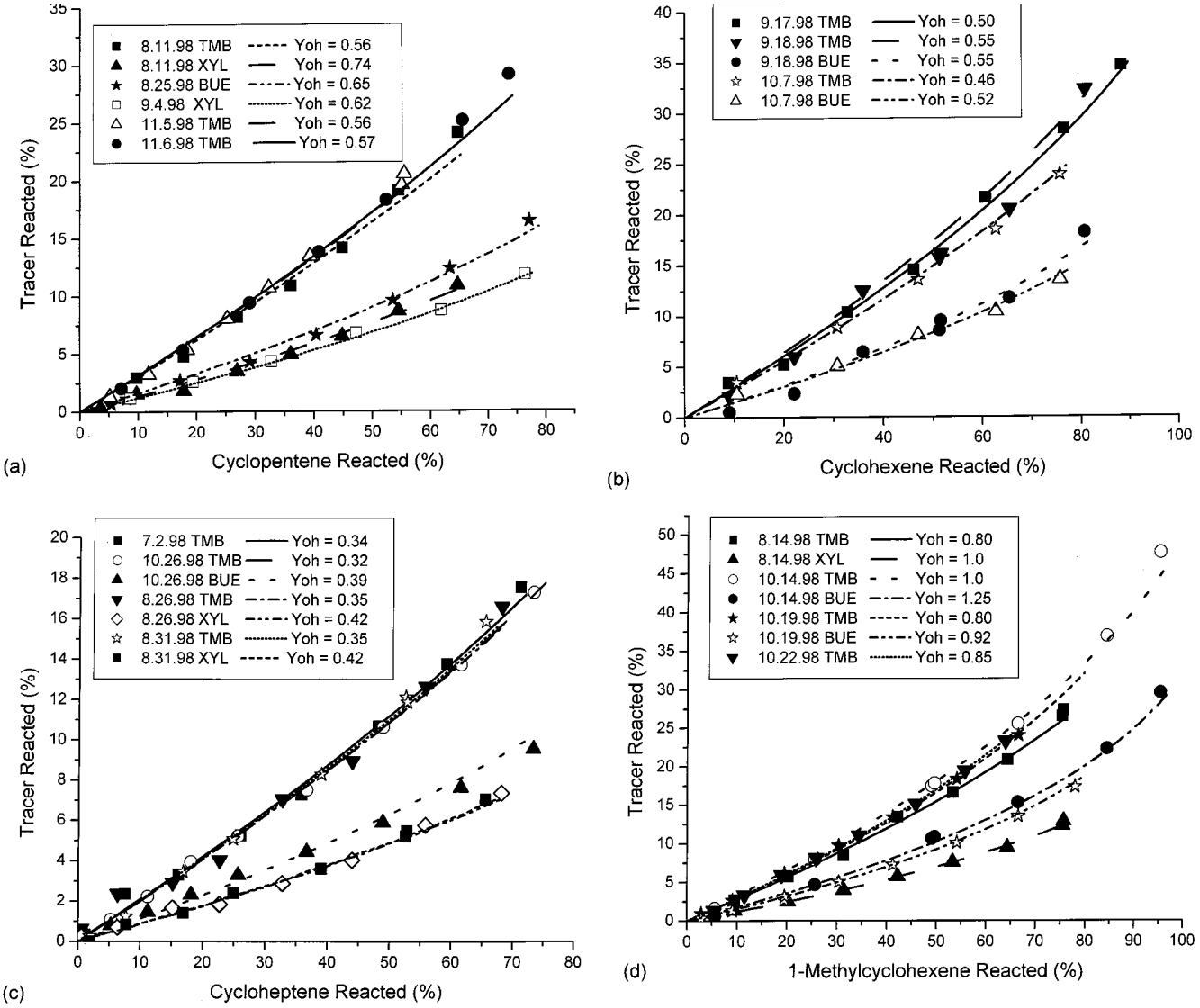

Figure 1. (a−d) Tracer reacted versus alkene reacted for several representative experiments. Symbols represent measurements and lines represent the model calculations, assuming the OH yield specified in the legends. The upper curves in each panel are 1,3,5-trimethylbenzene data and the lower curves are either di-*n*-butyl ether or *m*-xylene data.

TABLE 3: Calculated B3LYP/6-31G(d,p) Activation Enthalpies (kcal/mol) and Entropies (cal/(mol K)) for the Cycloreversion of Primary Ozonides (at 298 K)

	relative energies (kcal/mol)			
	Anti TS		*Syn* TS	
system	ΔH	ΔS	ΔH	ΔS
cis-2-butene	+15.6	−0.43	+18.6	−1.33
trans-2-butene	+17.5	+1.84	+17.3	+0.82
cyclopentene	+16.4	+1.11	+15.6	+0.82
cyclohexene	+13.6	+0.48	+15.5	+0.20
cycloheptene	+17.0	+0.46	+20.0	−0.03
1-methylcyclohexene	+15.8	+0.45	+12.9	+0.17
			+14.5	+0.44
			+15.8	+0.30

cleavage of the O−O bond (∼2.1 Å) is more advanced than cleavage of the C−C bond (∼1.9 Å). For all but 1-methylcyclohexene, the anti transition structures have nearly planar C−C−O−O torsional angles (170°−180°), whereas in the syn transition structures, the C−C−O−O torsional angles are significantly less planar (∼45°).

For *cis*-2-butene (Figure 2), the exo conformation of the primary ozonide is 0.8 kcal/mol more stable than the endo conformation. Cycloreversion to form anti acetaldehyde oxide has an activation barrier 3.0 kcal/mol lower than the barrier to form syn acetaldehyde oxide. The syn and anti transition structures have similar torsional angles about the breaking C−C bond ($|\tau$(C−C- - -C−C)| = 52° and 43°, respectively). For *trans*-2-butene (Figure 3), only one conformation of the primary ozonide is possible. Unlike the cis system, the *trans*-2-butene

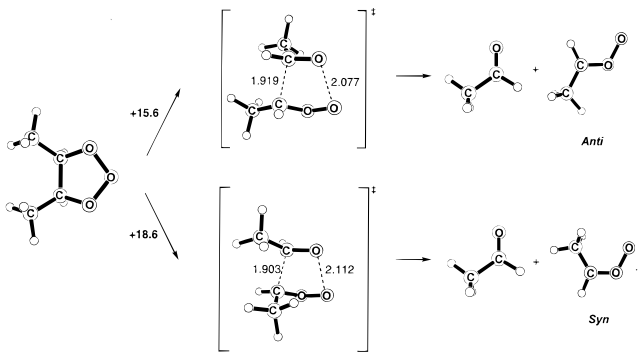

Figure 2. Cycloreversion of the *cis*-2-butene primary ozonide. Activation enthalpies (kcal/mol) and geometries of reactants, transition structures (bond lengths in Angstroms), and products from B3LYP/6-31G(d,p) calculations.

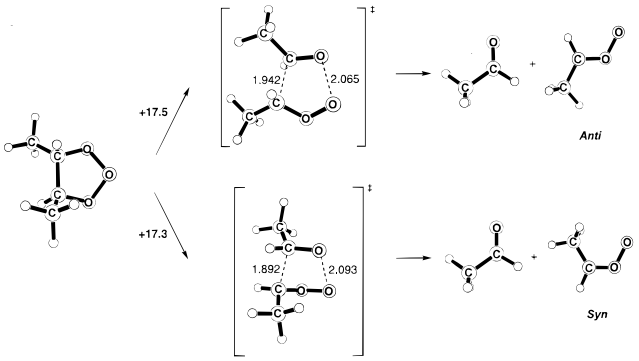

Figure 3. Cycloreversion of the *trans*-2-butene primary ozonide. Activation enthalpies (kcal/mol) and geometries of reactants, transition structures (bond lengths in Angstroms), and products from B3LYP/6-31G(d,p) calculations.

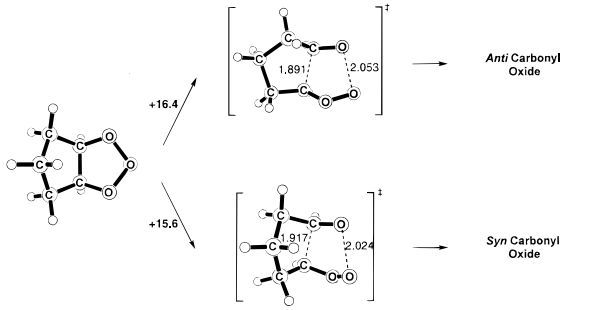

Figure 4. Cycloreversion of the cyclopentene primary ozonide. Activation enthalpies (kcal/mol) and geometries of reactants, transition structures (bond lengths in Angstroms), and products from B3LYP/6-31G(d,p) calculations.

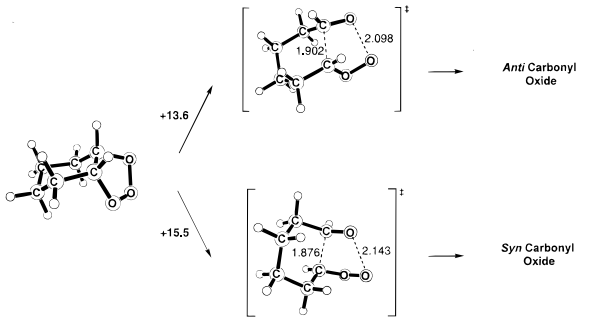

Figure 5. Cycloreversion of the cyclohexene primary ozonide. Activation enthalpies (kcal/mol) and geometries of reactants, transition structures (bond lengths in Angstroms), and products from B3LYP/6-31G(d,p) calculations.

syn and anti transition states have nearly the same energy. This is because the otherwise favored anti transition structure has a gauche Me−Me interaction ($|\tau$(C−C- - -C−C)| = 84°), whereas in the syn transition structure, the two methyl groups are nearly anti ($|\tau$(C−C- - -C−C)| = 164°).

For *cis*-2-butene and *trans*-2-butene, the B3LYP activation enthalpies predicted with the larger 6-311++G(d,p) basis set are all 3−4 kcal/mol lower than the corresponding 6-31G(d,p) values. Nevertheless, the differences in activation enthalpies predicted by the two basis sets are nearly identical. For *cis*-2-butene, the anti transition state is lower in enthalpy by 3.3 kcal/mol. For *trans*-2-butene, the syn transition state is lower in enthalpy by 0.1 kcal/mol. These results demonstrate the adequacy of the 6-31G(d,p) basis set.

Our B3LYP calculation predicts that *trans*-2-butene should generate more syn acetaldehyde oxide than *cis*-2-butene. The

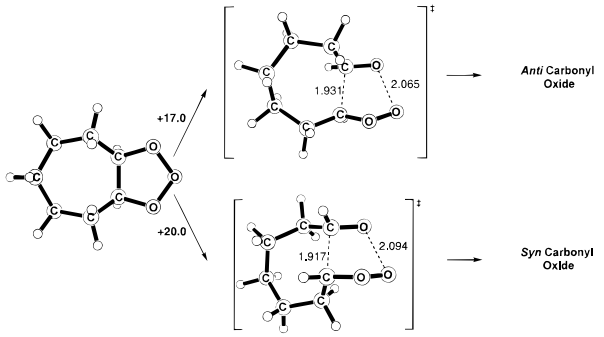

Figure 6. Cycloreversion of the cycloheptene primary ozonide. Activation enthalpies (kcal/mol) and geometries of reactants, transition structures (bond lengths in Angstroms), and products from B3LYP/6-31G(d,p) calculations.

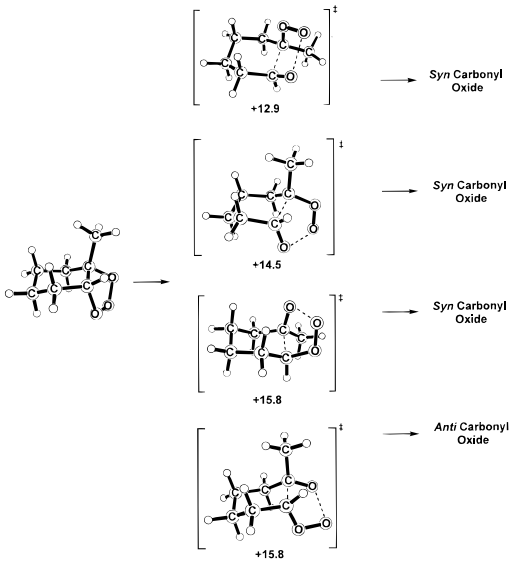

Figure 7. Cycloreversion of the 1-methylcyclohexene primary ozonide. Activation enthalpies (kcal/mol) from B3LYP/6-31G(d,p) calculations.

recent MP2 results of Rathman et al.[14] make a similar prediction. However, they predict that in *cis*-2-butene ozonolysis, the anti transition state is favored by 1.6 kcal/mol (versus our 3.0 kcal/mol), whereas in *trans*-2-butene ozonoylsis, the syn transition state is favored by 1.8 kcal/mol(versus our 0.2 kcal/mol syn preference). The trends are the same, but MP2 favors syn transition structures more than B3LYP.

The ozonolysis of acyclic alkenes is likely complicated by the participation of diradical pathways.[35] However, our B3LYP/6-31G(d,p) calculations indicate that the ozonolysis of cycloalkenes is dominated by closed-shell pathways. We found no minimum on the B3LYP surface corresponding to oxy−peroxy diradical intermediates from the conformationally rigid cyclopentene primary ozonide. Formation of gauche diradicals from the cyclohexene primary ozonide is possible, but further unimolecular reactions of these intermediates are predicted to be higher in energy (at least 16 kcal/mol above the primary ozonide) than both concerted cycloreversion transition states (Table 3).

For cyclopentene, the most stable conformation of the primary ozonide is endo/exo (the C−C−C flap is endo, and the O−O−O flap is exo, Figure 4). The exo/endo isomer, which is the most stable conformation on the AM1 surface,[12] is 0.6 kcal/mol higher in energy according to B3LYP. Formation of syn carbonyl oxides is kinetically favored by 0.8 kcal/mol (Table 3), similar to *trans*-2-butene.

For cyclohexene, the ozonide prefers the chair conformation (Figure 5), which forces the ozonide ring to have (approximately) C_2 symmetry, unlike the C_s primary ozonides of *cis*-2-butene (Figure 2), cyclopentene (Figure 4), and cycloheptene (Figure 6). For cyclohexene, the barrier against formation of the anti carbonyl oxide is 1.9 kcal/mol lower than the barrier against formation of the syn carbonyl oxide (Table 3). The cycloheptene primary ozonide prefers to adopt an exo chair conformation (Figure 6). The C−C−O−O dihedral angles are ±155.8°, almost identical to those for *cis*-2-butene primary ozonide (Figure 2). For cycloheptene, formation of the anti carbonyl oxide is kinetically favored by 3.0 kcal/mol (Table 3).

Finally, the 1-methylcyclohexene primary ozonide, like the unsubstituted system, prefers the chair conformation (Figure 7). The methyl−axial diequatorial ozonide is more stable than the equatorial methyl, axial−equatorial ozonide by 0.6 kcal/mol. B3LYP calculations predict that the primary ozonide cleaves regioselectively; the two lowest-energy transition states (with activation enthalpies of 12.9 and 14.5 kcal/mol) lead to the formation of stereoisomers of the disubstituted carbonyl oxide, which can undergo a 1,4-H shift to give OH. The structure that has the methyl group equatorial is more stable. Cleavage to give either the less-substituted syn or anti carbonyl oxide has an activation enthalpy of 15.8 kcal/mol.

In summary (Table 3), our B3LYP calculations reveal that as the cycloalkene ring is expanded from cyclopentene to cycloheptene, formation of the anti carbonyl oxide becomes increasingly favored.

Discussion

The quantum mechanical calculations provide a guide to the interpretation of the experimental data. There is relatively large barrier to interconversion of syn and anti carbonyl oxides ($\Delta H^{\ddagger} \sim 30$ kcal/mol).[17] The syn isomers can undergo a rapid 1,4-hydrogen shift ($\Delta H^{\ddagger} \sim 15$ kcal/mol), and the resulting vinyl hydroperoxide can easily cleave to OH plus alkoxy radicals ($\Delta H^{\ddagger} = 10-15$ kcal/mol). Because of the low barriers to these processes, it is likely that most syn carbonyl oxides formed will produce OH in gas-phase reactions.

Anti carbonyl oxides have relatively low energy pathways to dioxiranes ($\Delta H^{\ddagger} \sim 20$ kcal/mol). These are likely to undergo rearrangement to carboxylic acids or, at higher pressure, bimolecular oxygen atom transfer reactions upon collisions.[27,36] Thus, the anti species are expected to give OH inefficiently, if at all.

There is a relationship between the yield of OH detected in experimental studies and the relative ease of formation of syn carbonyl oxides according to calculations. Figure 8 shows a plot of the ln of the yield of hydroxyl radical formed from a given alkene versus the computed difference between activation enthalpies for formation of syn and anti carbonyl oxides from the decomposition of the primary ozonide. Clearly, when the formation of anti carbonyl oxide is favored, as with *cis*-2-butene and cycloheptene, the yield of OH is relatively low. When syn carbonyl oxide formation is favored, the yield of OH is high. The activation enthalpy differences vary from a 3 kcal/mol preference for syn to a 3 kcal/mol preference for anti carbonyl oxide formation, but there is a relatively small variation in OH yield, from 0.37 to 0.91. This result is consistent with the notion that the primary ozonides are formed in the gas phase by a very exothermic reaction and decompose promptly without significant vibrational relaxation. Although the ozonides are not thermally equilibrated, the relative rates of syn and anti carbonyl oxide formation do correlate with trends in relative activation enthalpies and not with relative activation entropies, which are nearly the same for the whole series.

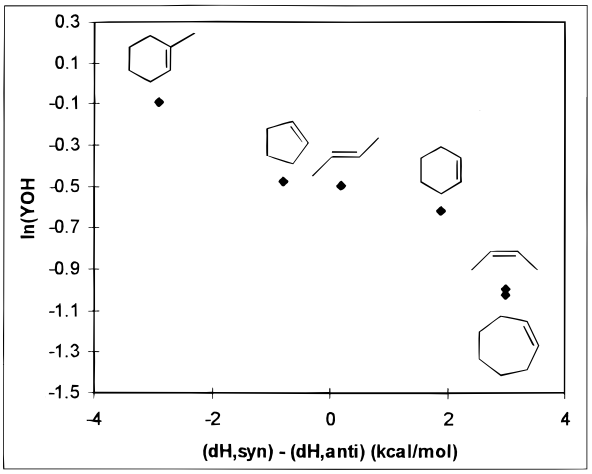

Figure 8. Plot of $\ln(Y_{OH})$ versus ($dH_{syn} - dH_{anti}$) using data from cyclopentene, cyclohexene, cycloheptene, 1-methylcyclohexene, *cis*-2-butene, and *trans*-2-butene. For 1-methylcyclohexene, $dH_{syn} - dH_{anti}$ was calculated using the lowest-energy syn transition state.

It is possible that there are other precursors of OH radical in addition to syn carbonyl oxides, such as vibrationally excited organic acids. Cremer et al.[27] have recently reported CCSD(T)/[4s3p2d1f/3s2p1d] calculations detailing a low-barrier pathway to the formation of formic acid from the parent carbonyl oxide:

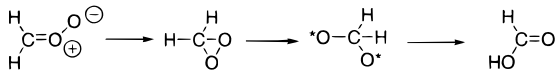

These calculations predict an enthalpy of formation (ΔH_f°(298 K)) for the parent carbonyl oxide of +27.0 kcal/mol. We can combine this single theoretical number with experimental data to test the idea that organic acids are OH radical precursors. Using this approach, we estimate that the formation of formic acid from carbonyl oxide is exothermic by −117.5 kcal/mol. The decomposition of formic acid to formyl radical and OH is endothermic by +100.5 kcal/mol. It is therefore thermodynamically possible to produce hydroxyl radical via a formic acid intermediate. However, the extremely high barrier against C−O bond homolysis suggests this process will be extremely slow. Moreover, Cremer et al.[27] predict that the decomposition of formic acid into CO and water is kinetically favored, with an activation enthalpy of +69.6 kcal/mol. The unlikelihood of formic acid affording OH has been previously noted by Gutbrod et al.[11] On the other hand, homolysis of the C−O bond of formic acid proceeds without an enthalpic barrier beyond the endothermicity. Hence, the transition state for this process will have a much larger density of states than the transition state leading to water and carbon monoxide. At high enough energies, decomposition of formic acid to give OH will therefore dominate. Thus, formic acid cannot be completely discounted as a source of OH.

The vinoxy radicals co-generated with OH in the proposed mechanism (R4) can themselves be sources of OH.[18] Laser-induced fluorescence experiments by Gutman and Nelson[37] and by Lorenz et al.[38] reveal OH to be one of the products of the reaction of the parent vinoxy radical with O_2. B3LYP/6-31G(d,p) calculations are in progress to explore the mechanism of these secondary reactions.

Although it would appear that the cycloalkenes are most directly comparable to cis acyclic olefins, the OH radical yields (Y_{OH}) indicate otherwise. Cyclopentene ($Y_{OH} = 0.62$) has an OH yield that is twice that of *cis*-2-pentene ($Y_{OH} \sim 0.30$)[39] and much higher than those of *cis*-2-butene ($Y_{OH} = 0.41$[10] and 0.37[39]) and *cis*-3-hexene ($Y_{OH} = 0.36$).[39] However, the OH yield from 1-methylcyclohexene ($Y_{OH} = 0.91$) is as large as that of the smaller acyclic compound, 2-methyl-2-butene ($Y_{OH} = 0.93$[40] and 1.0[39]). In this simple model, in which we assume syn carbonyl oxides generate OH quantitatively and anti carbonyl oxides do not, the OH yield for acyclic cis alkenes should not exceed 50%, as is observed. The proposed formation of an internal secondary ozonide (R6; vide supra[22]) should, if anything, further lower the OH yields for cycloalkenes compared with those for cis alkenes, which is opposite of what is observed.

Our B3LYP calculations give us some insight into the variation in OH yield with alkene structure. As first established by Cremer,[41] isolated syn acetaldehyde oxide is more stable than the anti form by ~3 kcal/mol due to homoaromaticity and two C−H- - -O electrostatic interactions in the syn geometry. In the cycloreversion transition states for the *cis*-2-butene primary ozonide, however, the stereochemical preference is reversed (Figure 2), with the anti geometry favored by ~3 kcal/mol. This reversal of stereoselectivity is likely due to a distortion of the syn carbonyl oxide fragment in the transition structure. The fragment is no longer planar ($|\tau(C-C-O-O)| = 45°$), which means both a loss of homoaromaticity and a loss of one of the C−H- - -O electrostatic interactions. The only remaining physical effect is steric interactions, which destabilize the syn carbonyl oxide fragment and the entire syn transition state. There is therefore an inherent kinetic preference for anti carbonyl oxide formation. However, our B3LYP calculations may overestimate the stability of the anti transition state.[14]

As already noted, the cycloheptene cycloreversion transition states are very similar structurally to the *cis*-2-butene transition states. It is therefore reasonable to expect that cycloheptene would have the same kinetic preference for formation of the anti carbonyl oxide, which is, in fact, the case: The anti transition structure is more stable than the syn transition structure by ~3 kcal/mol for both alkenes.

For cyclohexene ozonolysis, the preference for the anti transition state is lowered to 1.9 kcal/mol, and for cyclopentene ozonolysis, the syn transition state is favored by 0.8 kcal/mol. Unlike *trans*-2-butene ozonolysis, there are no apparent steric interactions about the breaking C−C bonds that would preferentially destabilize the anti transition structures for cyclohexene and cyclopentene. Calculations in progress seek to identify the mechanism by which small rings erode the inherent kinetic preference for anti carbonyl oxides.

Addition of a methyl substituent to cyclohexene perturbs the cycloreversion transition states in a predictable way (Figure 7). First, the methyl group, functioning as an electron donor, stabilizes the incipient partial positive charge on the carbon atom of the carbonyl oxide. This causes the two methyl-substituted carbonyl oxide transition states to be lowest in energy. Among these two, the structure that has the methyl group equatorial is lower by 1.6 kcal/mol. This value is close to the known free energy difference between axial and equatorial positioning (*A* value) of the methyl group in methylcyclohexane (1.7 kcal/mol).[42] For the two highest transition states, the 1.9 kcal/mol preference for the anti transition state seen in unsubstituted cyclohexene (Figure 5) is apparently balanced by a 1.9 kcal/mol preference for the equatorial methyl group, causing the two transition states to be equal in energy. The latter effect is also consistent with the literature *A* value for a methyl substituent.[42]

Our results also enable us to evaluate the least motion arguments of Bunnelle and Lee.[12] Our calculations show that the cyclopentene ozonide and transition structure have different preferred conformations, and the non-least-motion transition state is favored, contrary to the arguments of Bunnelle and Lee.[12] The ozonolysis of 1-methylcyclohexene (Figure 7) also violates the least-motion principle. As already stated, the primary ozonide prefers to have its methyl substituent axial by 0.6 kcal/mol. However, in the transition structures, the methyl group prefers to be equatorial by 1.6−1.9 kcal/mol.

The trend of decreasing OH yields with increasing size observed for the cyclopentene−cycloheptene series is also observed for terminal alkenes.[3,4] The pair 1-methylcyclohexene ($Y_{OH} = 0.91 \pm 0.20$) and α-pinene ($Y_{OH} = 0.70 \pm 0.17$[43]) also follows this trend. The interactions dictating these trends, however, may not be the same for cycloalkenes as for terminal alkenes or terpenes. Clearly, additional theoretical studies, including Rice−Ramsperger−Kassel−Marcus (RRKM) calculations, are warranted.

Acknowledgment. We thank the National Science Foundation (ATM-9629577 and CHE-9616772) and the Environmental Protection Agency for financial support of this work. Computational work was made possible by the UCLA Office of Academic Computing, the National Center for Supercomputing Applications, and the National Partnership for Advanced Computational Infrastructure. We thank Dr. A. S. Hasson of UCLA and Prof. R. Atkinson of the University of California at Riverside for helpful discussions.

Supporting Information Available: Electronic energies, optimized geometries, zero-point energies, and entropies of all calculated structures. This material is available free of charge via the Internet at http://pubs.acs.org.

References and Notes

(1) Guenther, A.; Hewitt, C. N.; Erickson, D.; Fall, R.; Geron, C.; Graedel, T.; Harley, P.; Klinger, L.; Lerdau, M.; McKay, W. A.; Pierce, T.; Scholes, B.; Steinbrecher, R.; Tallamraju, R.; Taylor, J.; Zimmerman, P. *J. Geophys. Res.* **1995**, *100*, 8873.

(2) Paulson, S. E.; Orlando, J. J. *Geophys. Res. Lett.* **1996**, *23*, 3727.

(3) Atkinson, R. *J. Phys. Chem. Ref. Data* **1997**, *26*, 215.

(4) Paulson, S. E.; Chung, M.; Hasson, A. *J. Phys. Chem. A* **1999**, *103*, 8125.

(5) Fraser, M. P.; Cass, G. R.; Simoneit, B. R. T.; Rasmussen, R. A. *Environ. Sci. Technol.* **1997**, *31*, 2356.

(6) Grosjean, D.; Fung, K. *J. Air Poll. Cont. Assn.* **1984**, *34*, 537.

(7) Jeffries, H. E. Photochemical Air Pollution. In *Composition, Chemistry, and Climate of the Atmosphere*; Singh, H. B., Ed.; Van Nostrand Reinhold: New York, 1995; pp 308.

(8) Henry, R. C.; Lewis, C. W.; Collins, J. F. *Environ. Sci. Technol.* **1994**, *28*, 823.

(9) Atkinson, R.; Tuazon, E. C.; Aschmann, S. M. *Environ. Sci. Technol.* **1995**, *29*, 1860.

(10) Atkinson, R.; Aschmann, S. M. *Environ. Sci. Technol.* **1993**, *27*, 1357.

(11) Gutbrod, R.; Schindler, R. N.; Kraka, E.; Cremer, D. *Chem. Phys. Lett.* **1996**, *252*, 221.

(12) Bunnelle, W. H.; Lee, S. *J. Am. Chem. Soc.* **1992**, *114*, 7577.

(13) Kawamura, S.; Yamakoshi, H.; Nojima, M. *J. Org. Chem.* **1996**, *61*, 5953.

(14) Rathman, W. C. D.; Claxton, R. A.; Rickard, A. R.; Marston, G. *Phys. Chem. Chem. Phys.* **1999**, *1*, 3981.

(15) Finlayson-Pitts, B. J.; Pitts, J. *Atmospheric Chemistry: Fundamentals and Experimental Techniques*; Wiley: New York, 1986.

(16) Bauld, N. L.; Thompson, J. A.; Hudson, C. E.; Bailey, P. S. *J. Am. Chem. Soc.* **1968**, *90*, 1822.

(17) Anglada, J. M.; Bofill, J. M.; Olivella, S.; Sole, A. *J. Am. Chem. Soc.* **1996**, *118*, 4636.

(18) Gutbrod, R.; Kraka, E.; Schindler, R. N.; Cremer, D. *J. Am. Chem. Soc.* **1997**, *119*, 7330.
(19) Niki, H.; Maker, P. D.; Savage, C. M.; Breitenback, L. P.; Hurley, M. D. *J. Am. Chem. Soc.* **1987**, *91*, 941.
(20) Donahue, N. M.; Kroll, J. H.; Anderson, J. G.; Demerjian, K. L. *Geophys. Res. Lett.* **1998**, *25*. 59.
(21) Olzmann, M.; Kraka, E.; Cremer, D.; Gutbrod, R.; Anderson, S. *J. Phys. Chem. A* **1997**, *101*, 9421.
(22) Hatakeyama, S.; Kobayashi, H.; Akimoto, H. *J. Phys. Chem.* **1984**, *88*, 4736.
(23) Paulson, S. E.; Fenske, J. D.; Sen, A. D.; Callahan, T. W. *J. Phys. Chem.* **1999**, *103*, 2050.
(24) Becke, A. D. *J. Chem. Phys.* **1993**, *98*, 5648.
(25) Hariharan, P. C.; Pople, J. A. *Chem. Phys. Lett.* **1972**, *66*, 217.
(26) Krishnan, R.; Frisch, M.; Pople, J. A. *Chem. Phys.* **1980**, *72*, 4244.
(27) Cremer, D.; Kraka, E.; Szalay, P. G. *Chem. Phys. Lett.* **1998**, *292*, 97.
(28) Frisch, M. J.; Trucks, G. W.; Schlegel, H. B.; Gill, P. M. W.; Johnson, B. G.; Robb, M. A.; Cheeseman, J. R.; Keith, T.; Petersson, G. A.; Montgomery, J. A.; Raghavachari, K.; Al-Laham, M. A.; Zakrzewski, V. G.; Ortiz, J. V.; Foresman, J. B.; Cioslowski, J.; Stefanov, B. B.; Nanayakkara, A.; Challacombe, M.; Peng, C. Y.; Ayala, P. Y.; Chen, W.; Wong, M. W.; Andres, J. O.; Replogle, E. S.; Gomperts, R.; Martin, R. L.; Fox, D. J.; Binkley, J. S.; Defrees, D. J.; Baker, J.; Stewart, J. P.; Head-Gordon, M.; Gonzalez, C.; Pople, J. A. *Gaussian 94*; Revision E. 2 ed.; Gaussian Inc.: Pittsburgh, PA, 1995.
(29) Frisch, M. J.; Trucks, G. W.; Schlegel, H. B.; Scuseria, G. E.; Robb, M. A.; Cheeseman, J. R.; Zakrzewski, V. J.; Montgomery, J. A.; Strapmann, R. E.; Durant, J. C.; Dapprich, S.; Millam, J. M.; Daniels, A. D.; Kudin, K. N.; Strain, M. C.; Farkas, O.; Tomasi, J.; Barone, V.; Cossi, M.; Cammi, R.; Mannucci, B.; Pomelli, C.; Adamo, C.; Clifford, S.; Ochterski, J.; Petersson, G. A.; Ayala, P. Y.; Cui, Q.; Morokuma, K.; Malick, D. K.; Rabuck, A. D.; Raghavachari, K.; Foresman, J. B.; Cioslowski, J.; Ortiz, J. V.; Stefanov, B. B.; Liu, J.; Liashenko, A.; Piskorz, P.; Komaromi, I.; Gomperts, R.; Martin, R. L.; Fox, D. J.; Keith, T.; Al-Laham, M. A.; Peng, C. Y.; Nanayakkara, A.; Gonsalez, C.; Challacombe, M.; Gill, P. M. W.; Johnson, B.; Chen, W.; Wong, M. W.; Andres, J. L.; Gonzalez, C.; Head-Gordon, M.; Replogle, E. S.; Pople, J. A. *Gaussian 98*; Revision A. 6 ed.; Gaussian, Inc.: Pittsburgh, PA, 1998.
(30) Paulson, S. E.; Sen, A. D.; Liu, P.; Fenske, J. D.; Fox, M. J. *Geophys. Res. Lett.* **1997**, *24*, 3193.
(31) Kramp, F.; Paulson, S. E. *J. Phys. Chem. A* **1998**, *102*, 2685.
(32) Kwok, E. S. C.; Atkinson, R.; Arey, J. *Environ. Sci. Technol.* **1996**, *30*, 1048.
(33) Jenkin, M. E.; Hayman, G. D. *J. Am. Chem. Soc., Faraday Trans.* **1995**, *91*, 1911.
(34) Lightfoot, P. D.; Cox, R. A.; Crowley, J. N.; Destriau, M.; Hayman, G. D.; Jenkin, M. E.; Moortgat, G. K.; Zabel, F. *Atmos. Environ.* **1992**, *26A*, 1805.
(35) Anglada, J. M.; Crehuet, R.; Bofill, J. M. *Chem. Eur. J.* **1999**, *5*, 1809.
(36) Adam, W.; Curci, R.; Edwards, J. O. *J. O. Acc. Chem. Res.* **1989**, *22*, 205.
(37) Gutman, D.; Nelson, H. H. *J. Phys. Chem.* **1983**, *87*, 3902.
(38) Lorenz, K.; Rhasa, D.; Zellner, R.; Fritz, B. *Ber. Bunsen-Ges. Phys. Chem.* **1985**, *89*, 341.
(39) Orzechowska, G. E.; Paulson, S. E., unpublished.
(40) Chew, A. A.; Atkinson, R. *J. Geophys. Res.* **1996**, *101*, 28649.
(41) Cremer, D. *J. Am. Chem. Soc.* **1979**, *101*, 7199.
(42) Lowry, T. H.; Richardson, K. S. *Mechanism and Theory in Organic Chemistry*, 3rd ed.; Harper Collins: New York, 1987.
(43) Paulson, S. E.; Chung, M.; Sen, A. D.; Orzechowska, G. *J. Geophys. Res.* **1998**, *103*, 25533.